EDN: BXTDRJ
УДК 535

Diagnostics of *Escherichia coli* Using Fabry-Perot Interference in Silicon Nanostructures of Various Morphologies

Mengyuan Wang*
Polina A. Rachishe§§
Daria A. Nazarovskaia†
Lomonosov Moscow State University
Moscow, Russian Federation
Pavel A. Domnin‡
Lomonosov Moscow State University
Moscow, Russian Federation
The Gamaleya National Research Center of Epidemiology and Microbiology
Moscow, Russian Federation
Ilia I. Tsiniaikin§
Aleksandra I. Efimova¶
Lomonosov Moscow State University
Moscow, Russian Federation
Svetlana A. Ermolaeva‖
The Gamaleya National Research Center of Epidemiology and Microbiology
Moscow, Russian Federation
Liubov A. Osminkina**
Kirill A. Gonchar††
Lomonosov Moscow State University
Moscow, Russian Federation

Received 10.08.2024, received in revised form 16.09.2024, accepted 24.10.2024

Abstract. This paper explores the potential for diagnosing bacterial presence in biological fluids using Fabry–Perot interference in silicon nanostructures with different morphologies. It compares the bacterial detection capabilities of porous silicon films and silicon nanowires, specifically focusing on the detection of *Escherichia coli* bacteria. The reflectance spectra of these nanostructures exhibit interference fringes resulting from Fabry–Perot interference. By analyzing changes in the effective optical thickness of the silicon nanostructures after bacterial deposition, the study concludes that silicon nanostructures with varying morphologies can be effectively used for bacterial detection.

Keywords: porous silicon, silicon nanowires, Escherichia coli, interference, sensorics.

*van.m17@physics.msu.ru §§ra4ishena@yandex.ru
†nazarovskayad@gmail.com https://orcid.org/0000-0001-8151-9602
‡paveldomnin6@gmail.com https://orcid.org/0000-0002-4130-1753
§ii.tcinyaykin@physics.msu.ru https://orcid.org/0000-0002-5820-8774
¶efimova@vega.phys.msu.ru https://orcid.org/0000-0002-3575-4481
‖drermolaeva@mail.ru https://orcid.org/0000-0003-3396-6816
**osminkina@physics.msu.ru https://orcid.org/0000-0001-7485-0495
††k.a.gonchar@gmail.com https://orcid.org/0000-0002-2301-2886

Citation: M. Wang, P.A. Rachishena, D.A. Nazarovskaia, P.A. Domnin, I.I. Tsiniaikin, A.I. Efimova, S.A. Ermolaeva, L.A. Osminkina, K.A. Gonchar, Diagnostics of *Escherichia coli* Using Fabry-Perot Interference in Silicon Nanostructures of Various Morphologies, J. Sib. Fed. Univ. Math. Phys., 2024, 17(6), 798–807. EDN: BXTDRJ.

Introduction

Escherichia coli (*E. coli*) is a bacterium commonly found in the lower intestine of warm-blooded organisms [1]. While most strains are harmless, certain serotypes, such as Enteropathogenic *E. coli*, can cause severe food poisoning and serious foodborne illnesses in their hosts [2]. Major sources of Shiga toxin-producing *E. coli* outbreaks include ground meat products [3], dairy products [4], and vegetables contaminated by fecal matter [5]. In many cases, the illness is self-limiting, but it can lead to life-threatening conditions, including Hemolytic Uremic Syndrome, particularly in young children and the elderly [6].

Several methods are used for the detection of *E. coli*, including surface-enhanced Raman spectroscopy (SERS) [7], polymerase chain reaction (PCR) [8], and colony-counting techniques [9]. However, each of these methods has significant limitations. For example, SERS requires additional sample modification, PCR demands stringent laboratory conditions, and colony-counting methods require 24–48 hours to produce results [10]. An alternative approach to bacterial detection involves exploiting light interference effects in thin porous films with different morphologies. In this method, white light is reflected at the top and bottom interfaces of the porous layer, generating Fabry–Perot interference. The frequency of this interference is determined by the film's effective optical thickness (EOT) [11].

Biosensors based on silicon nanostructures have a wide range of applications due to their high sensitivity and rapid response times. One such structure is thin films of porous silicon (pSi), which are produced by electrochemical (EC) etching of single-crystal silicon (c-Si) [12, 13]. The adsorption of various biomolecules or cells on the surface of these nanostructures alters the effective refractive index of pSi, leading to a shift in interference fringes and/or a change in their amplitude [12-16]. Detection capabilities can be further enhanced by modifying the pSi surface with antibodies or aptamers. It has been demonstrated that these functionalized structures, as well as those without surface modifications, can detect H1N1 viruses [14], *E. coli* bacteria in complex food industry process waters [15], and IgG binding [16].

Silicon nanowires (Si NWs) represent another type of silicon nanostructure commonly used in the creation of biosensors [17]. The most widely used method for fabricating Si NWs is metal-assisted chemical etching (MACE) [18]. Si NWs decorated with silver and/or gold nanoparticles have been successfully employed in the detection of bilirubin [19], internalin B [20], and *Listeria innocua* [21] using SERS. Additionally, nonspecific binding of the H1N1 virus to the surface of porous Si NWs (pSi NWs) has been demonstrated through changes in Fabry–Perot interference patterns [18]. By combining MACE with EC etching, double-etched porous silicon nanowire arrays have been fabricated, enabling the development of an impedance sensor for the H1N1 virus [22] and an interferometric sensor for *E. coli* bacteria [23].

This work presents the detection of *E. coli* using Fabry-Perot interference in silicon nanostructures with various morphologies. The detection capabilities of porous silicon and porous silicon nanowires for *E. coli* are compared.

1. Materials and methods

1.1. Fabrication of silicon nanostructures

Three different types of silicon nanostructures were prepared from p-type c-Si with crystallographic orientation (100) and resistivity 1–5 mΩ×cm. All samples were cleaned in C_2H_5OH before the fabrication:

1. ec-pSi.

   Electrochemically etched porous silicon (ec-pSi) was prepared using EC etching of c-Si in a solution of HF (48%) and C_2H_5OH with a 3:1 volume ratio, at an etching current density of 385 mA/cm^2 for 30 seconds.

2. sec-pSi.

   Sacrificial-etched porous silicon (sec-pSi) was prepared using sacrificial EC etching of c-Si. Initially, a c-Si wafer was etched in a solution of HF (48%) and C_2H_5OH with a 3:1 volume ratio for 30 seconds, at an etching current density of 300 mA/cm^2. The sample was then immersed in a 0.01 M NaOH solution, which dissolved the resulting porous structure. Following this, the EC etching process was repeated under the same conditions.

3. pSi NWs.

   PSi NWs were prepared using MACE method. Prior to etching, the c-Si wafer was cleaned in a 5 M HF solution for 1 minute to remove any SiO_2 from the surface. First, silver nanoparticles were deposited onto the c-Si surface by immersing the sample in a solution of $AgNO_3$ (0.02 M) and HF (5 M) with a 1:1 volume ratio for 15 seconds. In the second stage of MACE, the wafer coated with silver nanoparticles was placed in a solution of H_2O_2 (30%) and HF (5 M) with a 1:10 volume ratio for 20 minutes. Etching occurred in the areas coated with silver nanoparticles, which penetrated into the c-Si and formed filamentous Si NW structures. To remove the silver nanoparticles, the sample was subsequently placed in HNO_3 for 5 minutes.

1.2. Bacteria strains and growth conditions

E. coli strain JM109 maintained at -70°C in 10% glycerol, was obtained from N. F. Gamaleya National Research Center for epidemiology and microbiology. The bacteria were cultivated in the Luria–Bertani (LB, VMR Chemicals, USA) broth at 37°C with shaking at 180 rpm. Then, it was centrifugated at 4200 rpm for 10 min; supernatant was removed, and the bacteria were resuspended in sterile phosphate-buffered saline (PBS, pH 7.2-7.6, Sigma-Aldrich, USA). The resulting suspension was stored at 4°C.

1.3. Scanning electron microscopy

The structural properties of nanostructures were studied using a Carl Zeiss SUPRA 40 scanning electron microscope (SEM). To visualize *E. coli* on silicon nanostructures prior to measurements, the bacteria were immobilized on the substrates using a 2% glutaraldehyde solution in PBS for 90 minutes, followed by a dehydration process utilizing an ethanol series ranging from 50% to absolute ethanol [15].

1.4. Interferometric reflectance spectra acquisition

The reflectance spectra were measured in the spectral range 1500-5000 cm^{-1} using a Bruker IFS 66v/S spectrometer.

1.5. Adsorption process of *E. coli*

Silicon nanostructures were immersed in solution of *E. coli* with concentration of 10^6 CFU/mL for 15 minutes. The samples were then dried in a constant temperature oven at 37°C.

2. Results and discussions

SEM micrographs of the silicon nanostructures with *E. coli* are shown in Fig. 1. The thickness of the ec-pSi is approximately 8 μm (Fig. 1a), the sec-pSi is approximately 7 μm (Fig. 1d), and the pSi NWs is approximately 5.5 μm (Fig. 1g). Comparison of Fig. 1b and 1c with Fig. 1e and 1f

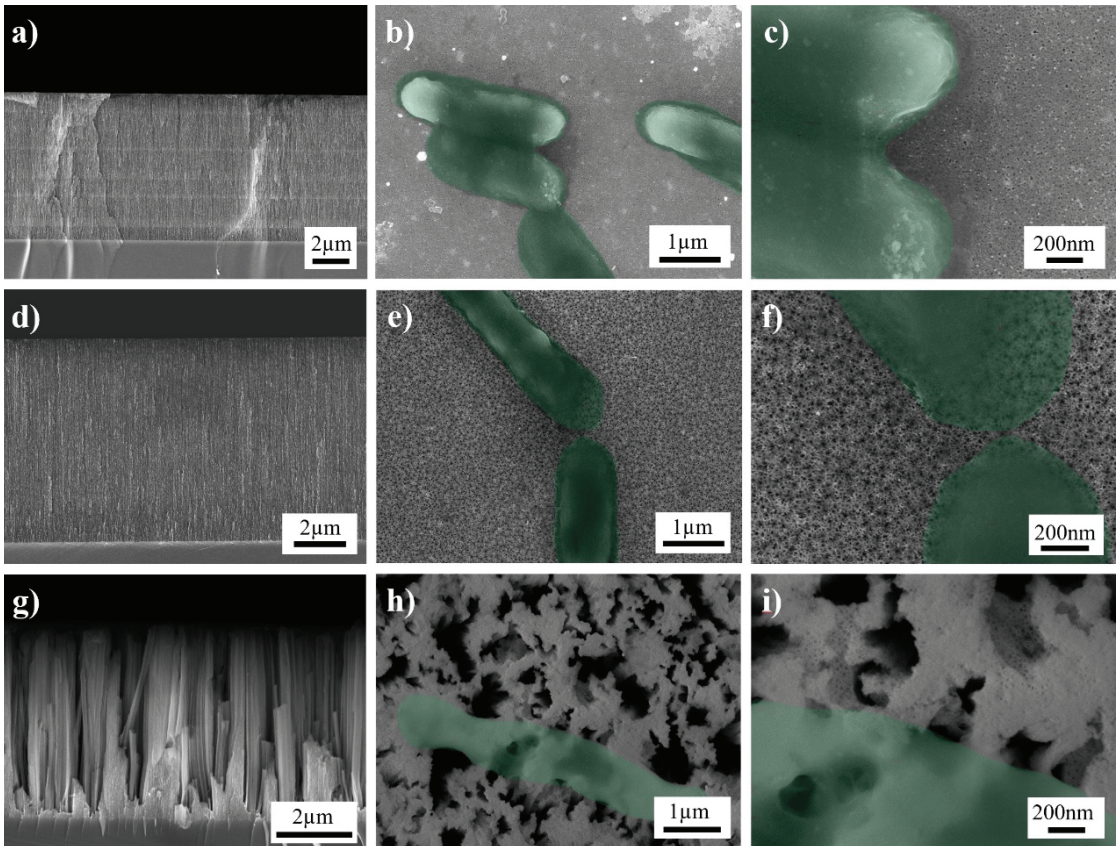

Fig. 1. SEM micrographs of silicon nanostructures with *E. coli*: a) side view of ec-pSi; b) top view of ec-pSi; c) enlarged top view of ec-pSi; d) side view of sec-pSi; e) top view of sec-pSi; f) enlarged top view of sec-pSi; g) side view of pSi NWs; h) top view of pSi NWs; i) enlarged top view of pSi NWs. In the top-view SEM micrographs of the silicon nanostructures, bacteria are pseudo-colored to facilitate observation

clearly shows that the pores in sec-pSi are more "open" than those in ec-pSi, which is attributed to the additional sacrificial EC etching. The pore size of the ec-pSi is approximately 5–10 nm and the pore size of the sec-pSi is approximately 10–15 nm. The distance between nanowires in the pSi NW sample is approximately 100–200 nm (Fig. 1h and 1i), which is significantly larger than the pore size of pSi. Thus, in pSi, bacteria settle only on the surface, while in pSi NWs, bacteria settle not only on the surface, but also partially in the pores between the nanowires. In the top-view SEM micrographs of the silicon nanostructures, bacteria are pseudo-colored to facilitate observation.

The reflectance spectra of nanostructures are characterized by the presence of interference fringes obtained as a result of Fabry-Perot interference (Fig. 2a). *EOT* of silicon nanostructures is calculated from the equation (1) [24]:

$$EOT = m\lambda = 2Ln_{eff}, \tag{1}$$

where m is the spectral order, λ is the wavelength of light, L is the thickness of silicon nanostructures and n_{eff} is the effective refractive index. Applying the fast Fourier transform (FFT) to the reflectance spectrum helps to find the difference in the *EOT* of silicon nanostructures without and with bacteria.

The reflectance spectra of ec-pSi both without and with *E. coli* at a concentration of 10^6 CFU/mL are shown in Fig. 2a. The *EOT* calculated from these reflectance spectra using FFT is presented in Fig. 2b.

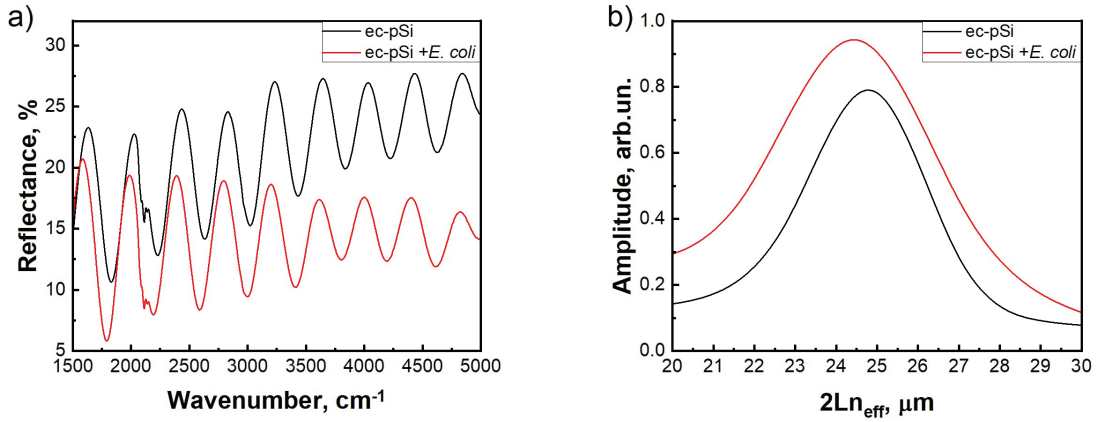

Fig. 2. a) Reflectance spectra of ec-pSi without and with *E. coli* at a concentration of 10^6 CFU/ml. b) Calculated *EOT* from the reflectance spectra using FFT

When *E. coli* was deposited on the surface of ec-pSi, the *EOT* decreased. This decrease can be attributed to two main effects. First, the presence of bacteria on the surface increased the overall thickness of the layer where interference fringes are observed. Second, the n_{eff} of the layer decreased because the bacteria were deposited only on the surface of the porous silicon film. Consequently, the upper part of the layer contained air and bacteria, rather than the silicon material. The combination of these effects — an increase in layer thickness and a decrease in n_{eff} — resulted in a reduced *EOT*.

The reflectance spectra of sec-pSi both without and with *E. coli* at a concentration of 10^6 CFU/mL are shown in Fig. 3a. The *EOT* calculated from these reflectance spectra using FFT is presented in Fig. 3b.

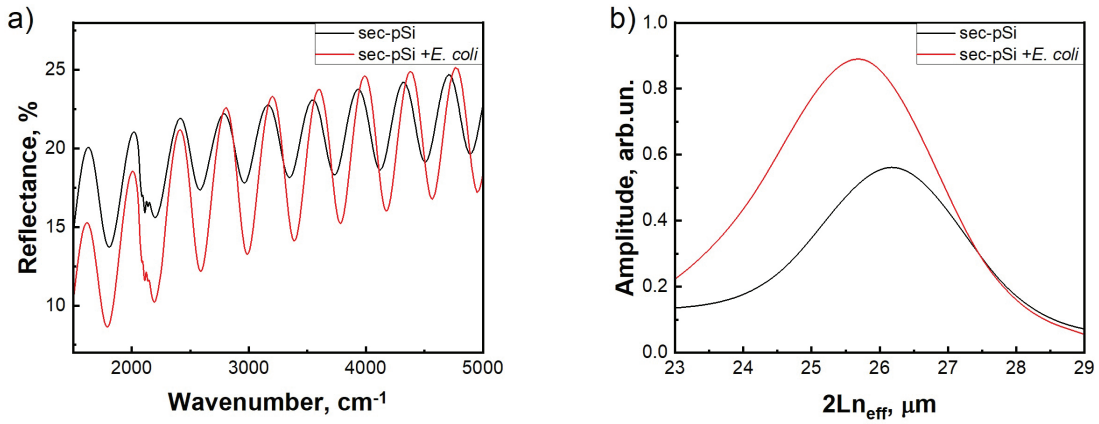

Fig. 3. a) Reflectance spectra of sec-pSi without and with *E. coli* at a concentration of 10^6 CFU/ml. b) Calculated *EOT* from the reflectance spectra using FFT

A similar decrease in *EOT* is observed during *E. coli* deposition for sec-pSi. However, the reduction in *EOT* for sec-pSi is more pronounced compared to ec-pSi. This greater decrease for sec-pSi can be attributed to the increased openness of the pores on the surface after sacrificial etching. This enhanced pore openness facilitates more efficient bacterial adsorption compared to ec-pSi, which was produced using the traditional method.

The reflectance spectra of pSi NWs both without and with E. coli at a concentration of 10^6 CFU/mL are shown in Fig. 4a. The EOT calculated from these reflectance spectra using FFT is presented in Fig. 4b.

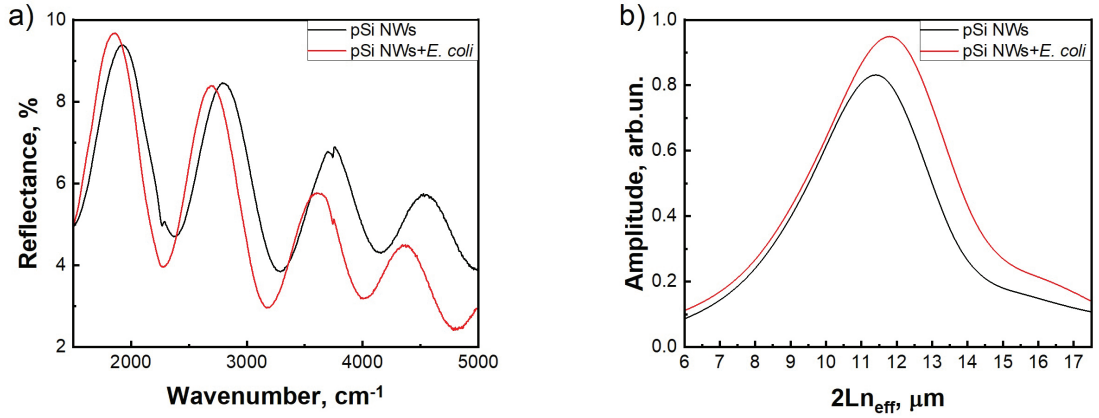

Fig. 4. a) Reflectance spectra of pSi NWs without and with *E. coli* at a concentration of 10^6 CFU/ml. b) Calculated *EOT* from the reflectance spectra using FFT

When *E. coli* were deposited on the surface of pSi NWs the *EOT* was increased. It can be explained that because of the big distance between nanowires the bacteria deposited not only on the surface, but also partially in the pores, which led to an increase of the *EOT* due to the growth of n_{eff} and L.

Conclusions

In this study, three different types of silicon nanostructures — traditional porous silicon film, sacrificially etched porous silicon film, and porous silicon nanowires were prepared and evaluated for *E. coli* detection using Fabry-Perot interference. Distinct effects on the *EOT* were observed depending on the type of nanostructure. For both pSi, the *EOT* decreased upon bacterial deposition. This reduction was due to the combined effects of an increased layer thickness and a decreased effective refractive index, as bacteria were mainly deposited on the surface of the small-pore-size pSi film, resulting in a layer predominantly composed of air and bacteria. However, the reduction in *EOT* for sec-pSi is more pronounced compared to ec-pSi, that can be attributed to the increased openness of the pores on the surface after sacrificial etching.

In contrast, the *EOT* increased for pSi NWs. This increase was attributed to the larger spacing between the nanowires, which allowed bacteria to be deposited not only on the surface but also partially within the pores. This deposition led to an increase in both the effective refractive index and the thickness of the layer, resulting in a higher EOT. The observed differences in *EOT* changes for pSi and pSi NWs underscore how the structural characteristics of the nanostructures affect bacterial interactions and their impact on optical properties.

Overall, this study confirms that all three types of silicon nanostructures — pSi, sacrificially etched pSi, and pSi NWs — are viable for detecting *E. coli* bacteria using Fabry–Perot interference. Each nanostructure exhibited distinct responses in *EOT* changes upon bacterial deposition, reflecting how structural differences influence sensor performance. Specifically, while pSi showed a decrease in *EOT*, pSi NWs exhibited an increase. These variations highlight that the effectiveness of bacterial detection can be significantly impacted by the nanostructure's morphology. Thus, this study not only validates the use of these silicon nanostructures for biosensing applications but also emphasizes the need to carefully consider structural characteristics to optimize sensor design for specific detection tasks.

The study was supported by the Russian Science Foundation, grant no. 22-72-10062 https://rscf.ru/en/project/22-72-10062/. M. Wang is grateful for the financial support provided by China Scholarship Council. The authors gratefully acknowledge the Educational and Methodological Center of Lithography and Microscopy and Research Facilities Sharing Center of Lomonosov Moscow State University for providing the equipment.

References

[1] O.Tenaillon, D.Skurnik, B.Picard, E.Denamur, The population genetics of commensal Escherichia coli, *Nature Reviews Microbiology*, **8(3)**(2010,) 207–217. DOI: 10.1038/nrmicro2298

[2] J.P.Nataro, J.B.Kaper, Diarrheagenic escherichia coli, Clinical microbiology reviews, **11**(1998), no. 1, 142–201. DOI: 10.1128/CMR.11.1.142

[3] R.L.Vogt, L. Dippold, Escherichia coli O157:H7 outbreak associated with consumption of ground beef, *Public Health Reports*, **120**(2005), no. 2, 174–178. DOI: 10.1177/003335490512000211

[4] R.Marier, J.G.Wells, R.C.Swanson, W.Callahan, I.Mehlman, An outbreak of enteropathogenic Escherichia coli foodborne disease traced to imported French cheese, *The Lancet*, **302**(1973), no. 7842, 1376–1378. DOI: 10.1016/S0140-6736(73)93335-7

[5] J.Castro-Rosas, J.F.Cerna-Cortes, etc., Presence of faecal coliforms, Escherichia coli and diarrheagenic E. coli pathotypes in ready-to-eat salads, from an area where crops are irrigated with untreated sewage water, *Int. J. Food Microbiol.*, **156**(2012), no. 2, 176–180. DOI: 10.1016/j.ijfoodmicro.2012.03.025

[6] J.P.Cramer, Enterohemorrhagic Escherichia coli (EHEC): Hemorrhagic Colitis and Hemolytic Uremic Syndrome (HUS), *Emerging infectious diseases, Clinical Case Studies, Academic Press, Elsevier Inc: Amsterdam, Netherlands*, (2014), 213–227. DOI: 10.1016/B978-0-12-416975-3.00017-0

[7] H.Jayan, H.Pu, D.W.Sun, Detection of bioactive metabolites in Escherichia coli cultures using surface-enhanced Raman spectroscopy, *Applied Spectroscopy*, **76**(2022), no. 7, 812–822. DOI: 10.1177/00037028221079661

[8] C.Bischoff, J.Luthy, M.Altwegg, F.Baggi, Rapid detection of diarrheagenic E. coli by real-time PCR, *Journal of microbiological methods*, **61**(2005), no. 3, 335–341. DOI: 10.1016/j.mimet.2004.12.007

[9] E.Bulard, A.Bouchet-Spinelli, P.Chaud, A.Roget, R.Calemczuk, S.Fort, T.Livache, Carbohydrates as new probes for the identification of closely related Escherichia coli strains using surface plasmon resonance imaging, *Analytical chemistry*, **87(3)**(2015), 1804–1811. DOI: 10.1021/ac5037704

[10] B.Thakur, G.Zhou, J.Chang, H.Pu, B.Jin, X.Sui, X.Yuan, C.-H.Yang, M.Magruder, J.Chen, Rapid detection of single E. coli bacteria using a graphene-based field-effect transistor device, Biosensors and Bioelectronics, **110**(2018), 16–22. DOI: 10.1016/j.bios.2018.03.014

[11] G.Shtenberg, E.Segal, Porous silicon optical biosensors. Handbook of Porous Silicon, *2nd ed.; Canham, L.; Springer International Publishing: Cham, Switzerland*, (2014), 857–868. DOI: 10.1007/978-3-319-05744-6_87

[12] A.Jane, R.Dronov, A.Hodges, N.H.Voelcker, Porous silicon biosensors on the advance, *Trends in biotech.*, **27**(2009), no. 4, 230–239. DOI: 10.1016/j.tibtech.2008.12.004

[13] V.S.Lin, K.Motesharei, K.P.Dancil, M.J.Sailor, M.R.Ghadiri, A Porous Silicon-Based Optical Interferometric Biosensor, *Science*, **278(5339)**(1997), 840–843. DOI: 10.1126/science.278.5339.840

[14] K.A.Gonchar, N.Yu.Saushkin, I.I.Tsiniaikin, A.A.Eliseev, A.S.Gambaryan, J.V.Samsonova, L.A.Osminkina, Virus diagnostics using Fabry-Perot interference films of macroporous silicon, *Optics and Spectroscopy*, **131**(2023), no. 9, 1221–1225. DOI: 10.61011/EOS.2023.09.57352.4933-23

[15] N.Massad-Ivanir, G.Shtenberg, N.Raz, C.Gazenbeek, D.Budding, M.P.Bos, E.Segal, Porous silicon-based biosensors: Towards real-time optical detection of target bacteria in the food industry, *Scientific Reports*, **6**(2016), 38099. DOI: 10.1038/srep38099

[16] K.-P.S.Dancil, D.P.Greiner, M.J.Sailor, A porous silicon optical biosensor: detection of reversible binding of IgG to a protein A-modified surface, *Journal of the American Chemical Society*, **121**(1999), no. 34, 7925–7930. DOI: 10.1021/ja991421n

[17] A.A.Leonardi, M.J.L.Faro, A.Irrera, Biosensing platforms based on silicon nanostructures: A critical review, *Analytica Chimica Acta*, **1160**(2021), 338393. DOI: 10.1016/j.aca.2021.338393

[18] K.A.Gonchar, S.N.Agafilushkina, etc., H1N1 influenza virus interaction with a porous layer of silicon nanowires, *Mater. Res. Express*, **7**(2020), 035002. DOI:10.1088/2053-1591/ab7719

[19] A.D.Kartashova, K.A.Gonchar, etc., Surface-enhanced Raman scattering-active gold-decorated silicon nanowire substrates for label-free detection of bilirubin, *ACS Biomater. Sci. Eng.*, **8**(2022), no. 10, 4175–4184. DOI: 10.1021/acsbiomaterials.1c00728

[20] K.A.Gonchar, E.A.Alekseeva, O.D.Gyuppenen, I.V.Bozhev, E.V.Kalinin, S.A.Ermolaeva, L.A.Osminkina, Optical express monitoring of internalin B protein of listeria monocytogenes pathogenic bacteria using SERS-active silver-decorated silicon nanowires, *Opt. Spectrosc.*, **130**(2022), no. 9, 521–526. DOI: 10.1134/S0030400X22110017

[21] D.A.Nazarovskaia, P.A.Domnin, etc., Advanced bacterial detection with SERS-active gold- and silver-coated porous silicon nanowires, *Bull. Russ. Acad. Sci. Phys.*, **87**(2023), Suppl. 1, S41–S46. DOI: 10.1134/S1062873823704385

[22] M.B.Gongalsky, U.A.Tsurikova, etc., Double etched porous silicon nanowire arrays for impedance sensing of influenza viruses, *Res. in Mat.*, **6**(2020), 100084. DOI: 10.1016/j.rinma.2020.100084

[23] M.B.Gongalsky, A.A.Koval, S.N.Schevchenko, K.P.Tamarov, L.A.Osminkina, Double etched porous silicon films for improved optical sensing of bacteria, *J. Electrochem. Soc.*, **164**(2017), no. 12, B581. DOI: 10.1149/2.1821712jes

[24] B.Rossi, Optics, 1st ed.; Addison-Wesley: Reading, MA, USA, 1957.

Диагностика *Escherichia coli* с помощью интерференции Фабри-Перо в кремниевых наноструктурах различной морфологии

Мэнюань Ван
Полина А. Рачишена
Дарья А. Назаровская
Московский государственный университет имени М. В. Ломоносова
Москва, Российская Федерация
Павел А. Домнин
Московский государственный университет имени М. В. Ломоносова
Москва, Российская Федерация
Национальный исследовательский центр эпидемиологии и микробиологии им. Н. Ф. Гамалеи
Москва, Российская Федерация
Илья И. Циняйкин
Александра И. Ефимова
Московский государственный университет имени М. В. Ломоносова
Москва, Российская Федерация
Светлана А. Ермолаева
Национальный исследовательский центр эпидемиологии и микробиологии им. Н. Ф. Гамалеи
Российская Федерация
Любовь А. Осминкина
Кирилл А. Гончар
Московский государственный университет имени М. В. Ломоносова
Москва, Российская Федерация

Аннотация. В данной статье исследуется возможность диагностики бактерий в биологических жидкостях с помощью интерференции Фабри–Перо в кремниевых наноструктурах с различной морфологией. Сравниваются возможности обнаружения бактерий с помощью плёнок пористого кремния и кремниевыми нанонитями, делая упор на обнаружение бактерий *Escherichia coli*. В спектрах отражения от этих наноструктур наблюдаются интерференционные полосы, возникающие в результате интерференции Фабри–Перо. Анализируя изменения эффективной оптической толщины кремниевых наноструктур после осаждения бактерий, в исследовании делается вывод, что кремниевые наноструктуры с различной морфологией могут эффективно использоваться для обнаружения бактерий.

Ключевые слова: пористый кремний, кремниевые нанонити, *Escherichia coli*, интерференция, сенсорика.